

Neural reinstatement reveals divided organization of fear and extinction memories in the human brain

Highlights

- MVPA of fMRI dissociates competing memories of fear and extinction in humans
- Memories of fear/extinction coded in dorsal/ventral prefrontal cortex, respectively
- Medial temporal lobe activity predicts locus of reinstatement in prefrontal cortex
- In a PTSD group, extinction memory misallocated to dorsal region coding for fear

Authors

Augustin C. Hennings, Mason McClay,
Michael R. Drew,
Jarrod A. Lewis-Peacock,
Joseph E. Dunsmaor

Correspondence

joseph.dunsmaor@austin.utexas.edu

In brief

How are competing memories of fear and safety stored in the brain? Using a hybrid episodic-associative memory design, Hennings et al. show dissociable reinstatement of emotional memories across the prefrontal cortex and hippocampus. Reinstatement of safety is dysregulated in PTSD, highlighting a neural correlate of maladaptive emotional learning.

Article

Neural reinstatement reveals divided organization of fear and extinction memories in the human brain

Augustin C. Hennings,^{1,2} Mason McClay,³ Michael R. Drew,^{1,2} Jarrod A. Lewis-Peacock,^{1,2,4,5} and Joseph E. Dunsmoor^{1,2,5,6,7,*}

¹Institute for Neuroscience, University of Texas at Austin, Austin, TX, USA

²Center for Learning and Memory, Department of Neuroscience, University of Texas at Austin, Austin, TX, USA

³Department of Psychology, University of California, Los Angeles, Los Angeles, CA, USA

⁴Department of Psychology, University of Texas at Austin, Austin, TX, USA

⁵Department of Psychiatry, Dell Medical School, University of Texas at Austin, Austin, TX, USA

⁶Twitter: [@joeydunsmoor](https://twitter.com/joeydunsmoor)

⁷Lead contact

*Correspondence: joseph.dunsmoor@austin.utexas.edu

<https://doi.org/10.1016/j.cub.2021.11.004>

SUMMARY

Neurobiological research in rodents has revealed that competing experiences of fear and extinction are stored as distinct memory traces in the brain. This divided organization is adaptive for mitigating overgeneralization of fear to related stimuli that are learned to be safe while also maintaining threat associations for unsafe stimuli. The mechanisms involved in organizing these competing memories in the human brain remain unclear. Here, we used a hybrid form of Pavlovian conditioning with an episodic memory component to identify overlapping multivariate patterns of fMRI activity associated with the formation and retrieval of fear versus extinction. In healthy adults, distinct regions of the medial prefrontal cortex (PFC) and hippocampus showed selective reactivation of fear versus extinction memories based on the temporal context in which these memories were encoded. This dissociation was absent in participants with posttraumatic stress disorder (PTSD) symptoms. The divided neural organization of fear and extinction may support flexible retrieval of context-appropriate emotional memories, while their disorganization may promote overgeneralization and increased fear relapse in affective disorders.

INTRODUCTION

Maintaining separate and competing memories of threat and safety is key to adaptive behavior. The inability to maintain memories of safety to overcome threat associations characterizes affective disorders, such as posttraumatic stress disorder (PTSD).^{1,2} Neurobiological research using Pavlovian conditioning shows neural ensembles within and between dissociable regions organize the encoding, storage, and retrieval of fear (threat) and extinction (safety) memory.^{3–6} This research confirms early theories—dating back to the time of Pavlov—that extinction is an active learning process that generates a secondary memory of safety for a particular stimulus that is stored in parallel to the memory of fear for that stimulus. In the rodent brain, these memory traces are separated into discrete neural ensembles with distinct pathways between regions of the medial temporal lobe (MTL) and subdivisions of the medial prefrontal cortex (mPFC).^{7–11} A similar neural organization has been identified in humans using functional magnetic resonance imaging (fMRI),^{12–15} although the mechanisms by which fear and extinction memories are segregated into separate regions in the human brain remain unclear. Here, we use multivariate pattern analysis (MVPA) of fMRI data to isolate spatially distributed patterns of overlapping activity unique to the encoding and retrieval of fear versus extinction memories. We compare these neural

signatures between healthy adults and individuals with PTSD symptoms, for which the ability to organize separable fear and extinction memories is presumably dysregulated.^{16–18}

Identifying quantifiable memory traces in the brain can be challenging; memories are widely distributed within and across discrete brain regions, memories change over time, and not all experiences induce a persistent neural change. Fear conditioning is an ideal model to investigate the neural representations of memory, as it rapidly induces stable and persistent associative memory with objective behavioral correlates. One of the most important discoveries in the neuroscience of associative learning was the localization of neural circuits selective for the formation and retrieval of fear versus extinction. In the MTL, sparse coding allows for fear and extinction to exist simultaneously in the same structures,^{19,20} with a more stark division in the mPFC. The prelimbic cortex (PL), homologous to the human dorsal anterior cingulate cortex (dACC), is activated during learning and retrieval of fear associations,^{21–23} whereas the infralimbic cortex (IL), homologous to the human ventromedial PFC (vmPFC), is a critical site of extinction memory formation and retrieval.^{24–26} These areas interact dynamically with the amygdala and hippocampus (HC) to either express or suppress conditioned fear.^{10,27}

Human neuroimaging has successfully translated evidence from rodents that the dACC is among the most consistently

active regions during fear conditioning.^{13,28} However, it is far less clear in humans whether this region is also the site of long-term storage and retrieval of acquired fear memories. Moreover, neuroimaging evidence of vmPFC involvement in extinction is surprisingly scant. While some studies have been able to show a role for the vmPFC,^{12,14,29,30} a robust meta-analysis has revealed that the vmPFC is *not* among a collection of regions that are consistently active during extinction learning.³¹ This inconsistency between animal neurophysiology and human neuroimaging has been a puzzle and limits the translational utility of advances in extinction research in rodents.

A major hurdle to translating animal neurophysiology to human neuroimaging is a methodology to “label” brain activity uniquely associated with memories of either fear or extinction. In rodents, state-of-the-art advances in activity-dependent labeling separate these memory traces by measuring the overlap in activity during acquisition and retrieval in collections of neurons, termed engrams.^{19,32} An analogous analytic approach in human neuroimaging involves correlating overlapping multivariate patterns of activity during memory encoding and retrieval. The match between activity patterns in distributed voxels during encoding and retrieval provides an index of memory fidelity, albeit not at the cellular level. This neuroimaging technique has been widely applied to the study of human episodic memory.^{33–37} Whether this technique can be leveraged to isolate associative memory traces of fear and extinction in the human brain, based on memory encoding context, has not been tested.

We use a 2-day hybrid conditioning and episodic memory design that incorporates trial-unique (i.e., non-repeating) semantic exemplars as conditioned stimuli (CS) during fear conditioning and extinction on day 1.³⁸ On day 2, participants undergo a surprise memory test for the unique CS exemplars encoded during conditioning and extinction. This hybrid design overcomes inherent obstacles to typical conditioning protocols. That is, typically the same CS (e.g., a colored shape) is repeated across all experimental phases. Consequently, it is only possible to measure retrieval of either the putative fear or extinction memory at test, but not both. In our hybrid design, we simultaneously isolate specific episodes associated with fear and extinction (comparable to activity-dependent labeling in murine studies) and quantify the overlap in patterns of activity for each CS as a function of the temporal context in which the CS was encoded. In this way, we quantify whether and how these competing memories distinctly organize into separable patterns of activity in each participant and in a single experiment. This design innovation allows us to leverage technical advances in multivariate analyses of neuroimaging data for human episodic memory within the conceptual framework of functional labeling from rodent neurophysiology.

We hypothesized that the healthy adult brain organizes and maintains separable mnemonic representations of fear and extinction, and we sought to distinguish these memories based on the temporal context in which the memory was originally formed. We hypothesized that fear memories would be represented similarly in healthy adults and individuals with posttraumatic stress symptoms (PTSSs). However, based on extensive evidence of maladaptive processing and return of fear in PTSD,^{39–41} we hypothesized that neural organization of extinction memories would differ between groups.

RESULTS

Figure 1 provides an overview of analytic approach. Participants encoded trial-unique pictures of animals and tools before, during, and after fear conditioning. One semantic category (animals or tools, counterbalanced) served as CS+ and co-terminated with an electrical shock during fear conditioning (50% reinforcement), while the other category never paired with shock (CS−). Extinction learning immediately followed conditioning, during which no shocks were delivered. Participants returned 24 h later for a surprise recognition memory test composed of all the CSs plus novel lures.

Behavioral results

Explicit and implicit measures of learning

As we previously reported,⁴² the success of fear conditioning and extinction learning was assessed by skin conductance responses (SCRs) and trial-by-trial shock expectancy (yes or no 2-alternative forced choice [AFC]). Analyses focused on differential responding (i.e., CS+ > CS− differences; **Figure 2A**; see **Figure S1** for full behavioral results). During conditioning, groups exhibited significant CS+ > CS− responses for both SCR (healthy: $t_{(23)} = 4.22$, $p = 3.25e-4$; PTSS: $t_{(23)} = 3.17$, $p = 4.31e-3$) and shock expectancy (healthy: $t_{(23)} = 14.3$, $p = 6.16e-13$; PTSS: $t_{(23)} = 7.62$, $p = 9.89e-8$). The success of extinction learning was assessed by comparing differential responses from conditioning to the second half of extinction (“late extinction”). Both groups displayed significant reductions in differential SCR (healthy: $t_{(21)} = -2.6$, $p = 0.017$; PTSS: $t_{(21)} = -2.86$, $p = 9.34e-3$) and shock expectancy (healthy: $t_{(23)} = -4.33$, $p = 2.46e-4$; PTSS: $t_{(23)} = -3.66$, $p = 1.29e-3$). Importantly, there were no significant differences in behavioral responses between groups during either conditioning (SCR: $t_{(46)} = 0.63$, $p = 0.53$; expectancy: $t_{(46)} = 1.23$, $p = 0.22$) or late extinction (SCR: $t_{(42)} = 0.49$, $p = 0.63$; expectancy: $t_{(46)} = 0.69$, $p = 0.50$). Together, these results demonstrate successful and equivalent fear conditioning and within-session extinction in both groups.

Recognition memory

Overall, performance on the recognition memory test replicated previous behavioral findings,^{43–45} in that memory was better for CS+ items compared to CS− from all phases and overall higher for conditioning compared to other phases. Here, we report an analysis of high-confidence hit rates to test for differences in episodic memory between groups. A mixed-effects ANOVA of high-confidence hit rates revealed no significant main effect of group ($F_{1, 46} = 1.37$; $p = 0.25$), no significant two-way interactions between group and either CS type or encoding context, and no significant three-way interaction (all $p \geq 0.44$). These results indicate that explicit recognition memory for the CS items was not different between groups.

Emotional memory reinstatement in the mPFC

The analyses here focus on the overlap of multi-voxel fMRI activity patterns of items from encoding to retrieval (i.e., encoding–retrieval similarity), irrespective of memory performance. The voxelwise patterns of activity elicited by each CS item during the recognition memory test were correlated with the patterns of activity elicited by those same CS items when they were initially encoded during either the pre-conditioning, fear

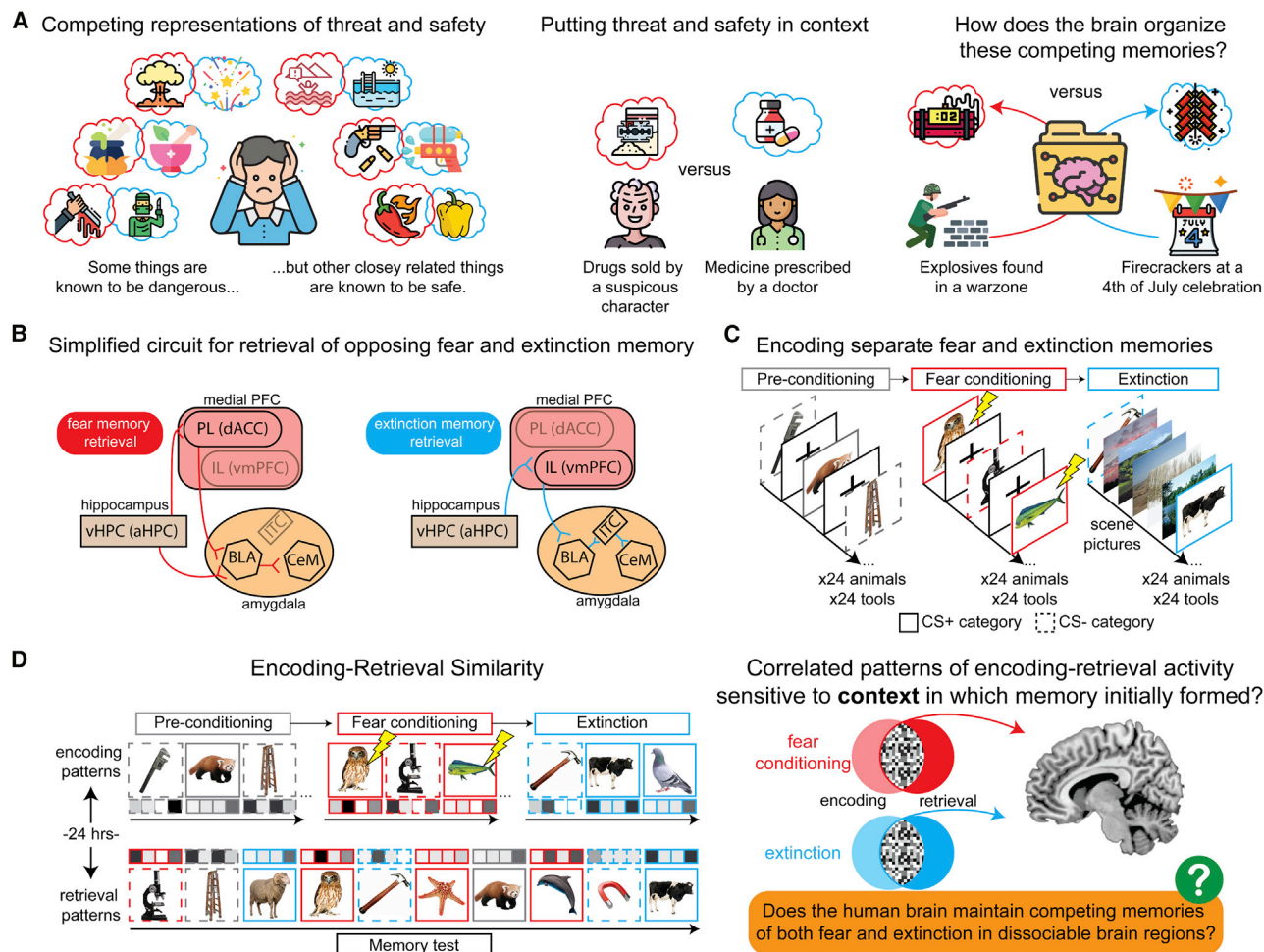


Figure 1. Divided organization of fear and extinction memories in the human brain

(A) Schematic overview. People maintain competing representations of threat and safety for closely related stimuli and often retrieve the appropriate association given the context. Disorganization between competing memories leads to maladaptive responses in harmless situations.

(B) Simplified circuit diagrams of fear and extinction memory retrieval, highlighting the interactions between the MTL and mPFC. Parentheses indicate human homologs of rodent neural structures.

(C) Associative learning (day 1). Semantic categories served as the CS+ and CS-; each trial was a unique, non-repeating, category exemplar.

(D) Encoding-retrieval similarity analysis. 24 h after learning, participants completed a surprise recognition memory test during fMRI. Neural reinstatement was measured by correlating encoding and retrieval patterns in a given ROI.

aHc, anterior hippocampus; BLA, basolateral amygdala; CeM, central nucleus of the amygdala; ITC, intercalated cells; vHc, ventral hippocampus.

conditioning, or extinction phase. To control for item-level reinstatement effects, these correlations were Fisher Z transformed and then the average correlation of CS- trials was subtracted from the average correlation of the CS+ trials from the same encoding context. This analysis focused on distinct mPFC subregions motivated by rodent work:^{22,24} the dACC and vmPFC, which were defined *a priori*.

In healthy adults, the dACC exhibited greater reinstatement for CS+ items (compared to CS- items) that were encoded during fear conditioning (Figure 2B, top; difference = 0.22; 95% confidence interval [CI] = [0.16, 0.28]; $p_{\text{FDR}} = 4.62\text{e-}12$). This finding accords with rodent models that show the PL is involved in both the learning and retrieval of long-term fear memories. Reinstatement in the dACC was stronger for fear memories (CS+ – CS- from conditioning) than for extinction memories (CS+ – CS-

from extinction; 0.21; [0.12, 0.29]; $p_{\text{FDR}} = 6.26\text{e-}6$). Moreover, this region did not show any preferential CS+ reinstatement of extinction memories (0.014; [−0.046, 0.075]; $p_{\text{FDR}} = 0.64$) or pre-conditioning memories (0.006; [−0.054, 0.066]; $p_{\text{FDR}} = 0.84$). In sum, the dACC appears highly specialized for the reinstatement of fear memories in the healthy adult brain. In the vmPFC, there was reinstatement of both fear memories (0.074; [0.013, 0.134]; $p_{\text{FDR}} = 0.033$) and extinction memories (0.113; [0.053, 0.173]; $p_{\text{FDR}} = 9.20\text{e-}4$). There was no preferential CS+ reinstatement of pre-conditioning memories (−0.020; [−0.081, 0.040]; $p_{\text{FDR}} = 0.50$). Notably, there was a significant double dissociation in the selective reinstatement of fear and extinction memories between these two regions (significant CS type × encoding context × region of interest [ROI] interaction; $\chi^2_{(1)} = 16.2$; $p = 5.71\text{e-}5$). Specifically, there was stronger reinstatement of fear memories in the

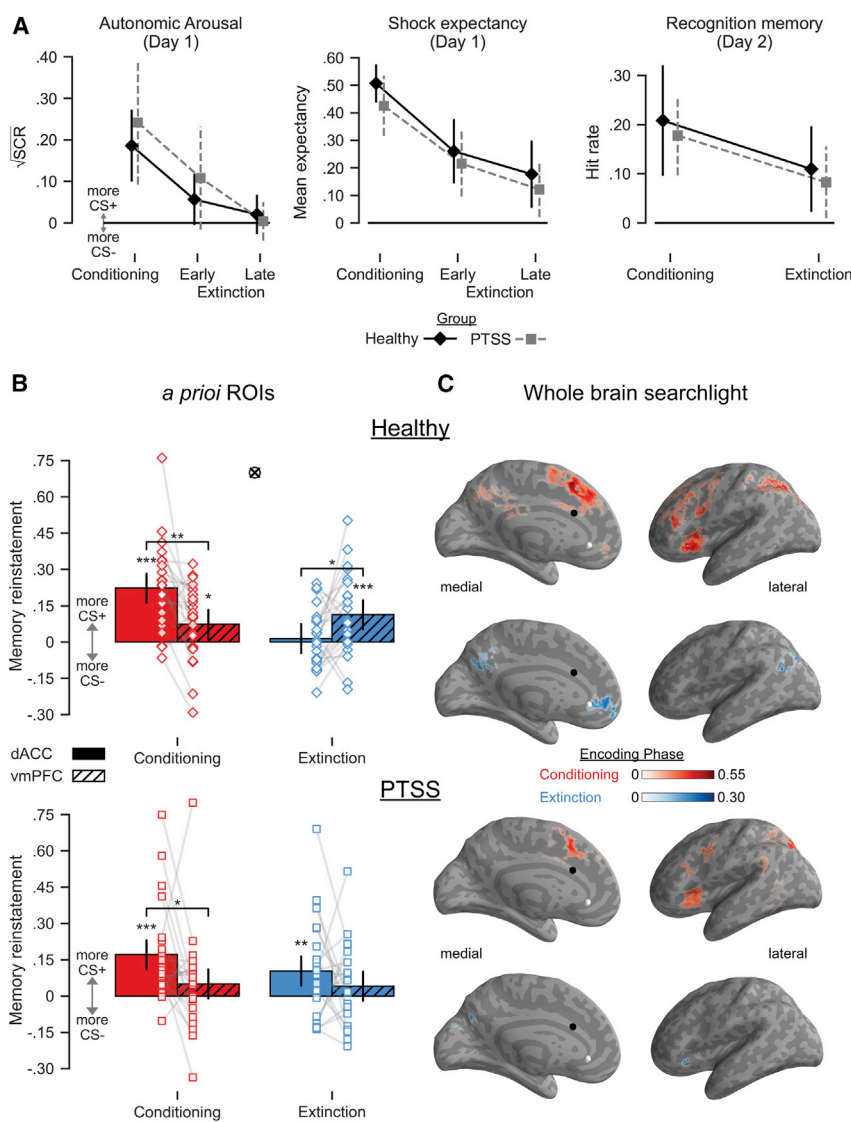


Figure 2. Dissociable reinstatement of emotional memories

Error bars indicate the 95% CI of the CS+ – CS- difference. ***p < 0.001; **p < 0.01; *p < 0.05; false discovery rate (FDR) corrected.

(A) Behavior. SCR and shock expectancy from conditioning and extinction (split by half) on day 1 are replicated from Hennings et al.⁴² 24 h delayed recognition memory hit rates are also shown. Critically, no group behavioral differences were observed for day 1 associative learning or 24 h recognition memory.

(B) Reinstatement in *a priori* ROIs. Top: healthy adults exhibited a significant double dissociation of emotional memory reinstatement in the mPFC. Bottom: in PTSS, the dACC displayed significant emotional memory reinstatement for both conditioning and extinction, revealing a misallocation of extinction memories.

(C) Whole-brain analysis. A whole-brain searchlight calculated reinstatement around each voxel. Medial and lateral views of the inflated left hemisphere are shown; results were qualitatively similar across hemispheres. Heatmaps show average emotional reinstatement for conditioning (red) and extinction (blue), threshold at p < 0.001 one-sided for CS+ > CS- with a clusterwise threshold of p < 0.05. The centers of *a priori* ROIs are marked on the cortical surface for the dACC (black) and vmPFC (white).

dACC relative to the vmPFC (0.149; [0.064, 0.234]; p_{FDR} = 0.002) and stronger reinstatement of extinction memories in the vmPFC relative to the dACC (0.099; [0.014, 0.184]; p_{FDR} = 0.031). Altogether, in healthy adults, discrete regions of the mPFC exhibited a double dissociation in the reinstatement of fear and extinction, as identified by the temporal context in which the memories were formed (see Figure S2 for a complementary analysis highlighting the importance of temporal context).

As with healthy adults, individuals with PTSS also exhibited greater reinstatement in the dACC for CS+ items encoded during conditioning (Figure 2B, bottom; 0.171; [0.111, 0.231]; p_{FDR} = 1.53e-7), and reinstatement of fear memories was stronger in the dACC relative to the vmPFC (0.121; [0.036, 0.206]; p_{FDR} = 0.011). There was also a lack of preferential CS+ reinstatement in the dACC for pre-conditioning memories (0.032; [-0.028, 0.092]; p_{FDR} = 0.30). This pattern of fear memory reinstatement is consistent with results in healthy adults and suggests that individuals with PTSS do not exhibit a fear learning deficit. Unlike the healthy adult group, however, the PTSS group showed

reinstatement for CS+ items encoded during extinction in the dACC (0.103; [0.043, 0.164]; p_{FDR} = 0.002). These results suggest that individuals with PTSS misallocated extinction memories, as information encoded in the extinction context was reinstated in the same region involved in the formation and retrieval of fear memories. In the vmPFC, surprisingly, there was greater reinstatement of CS- items (relative to CS+ items) encoded prior to fear conditioning (-0.079; [-0.139, -0.019]; p_{FDR} = 0.024).

In contrast to the healthy adult group, there was no evidence of greater reinstatement for CS+ items encoded during either conditioning (0.050; [-0.010, 0.110]; p_{FDR} = 0.10) or extinction (0.041; [-0.020, 0.101]; p_{FDR} = 0.19) in the vmPFC. The significant double dissociation of fear and extinction memory reinstatement we observed in the healthy adults was not present in the PTSS group (no significant CS type × encoding context × ROI interaction; $\chi^2_{(1)} = 0.88$; p = 0.35). Thus, while individuals with PTSS exhibit normal reinstatement of fear memories in the dACC, this group did not exhibit any reinstatement of extinction memories in the vmPFC. Instead, reinstatement was observed in the dACC, which suggests a misallocation of extinction memories to a brain region that preferentially codes for fear.

These results show that healthy adults and individuals with PTSS display markedly different patterns of emotional memory reinstatement across the mPFC, particularly for extinction memories. Using linear contrasts, we directly tested whether the observed pattern significantly differed between groups by comparing reinstatement in vmPFC versus dACC for each phase.

The groups did not differ in their expression of fear memory reinstatement across the mPFC (0.028; [−0.092, 0.148]; $p_{FDR} = 0.65$); however, as expected, there was a significant difference between healthy adults and individuals with PTSS in extinction memory reinstatement across the mPFC (0.161; [0.041, 0.282]; $p_{FDR} = 0.017$).

Emotional memory reinstatement outside *a priori* cortical ROIs

Compared to similar work in rodents, a comparative advantage of fMRI is the ability to observe the entire brain. To complement the results from the *a priori* ROIs, we conducted an exploratory whole-brain searchlight for emotional memory reinstatement (Figure 2C). In healthy adults, this analysis revealed additional brain regions that exhibit reinstatement of fear or extinction memories (see Table S1 for full list of cluster locations). In addition to the dACC, fear memories were reinstated in the anterior insula, a region consistently implicated in human fear memory.²⁸ For the reinstatement of extinction memories, the largest cluster was found in vmPFC. Other cortical regions, including the medial frontal gyrus and precuneus, exhibited reinstatement for both fear and extinction memories. Individuals with PTSS were like healthy adults—with reinstatement of fear memories in large clusters corresponding to the dACC, bilateral insula, and other cortical regions. For extinction memories, we observed significant clusters in the cuneus, as well as in bilateral insula. See Figure S3 for post hoc ROI analyses of emotional memory in the anterior insula and precuneus.

Emotional memory reinstatement in the medial temporal lobe

The amygdala and HC are core components of the neurocircuitry involved in the acquisition and retrieval of both fear and extinction memories. The HC in particular exerts contextual control over memory retrieval.¹⁷ Emerging neurobiological models in rodents indicate that different subfields along the long axis of the HC serve discrete functions in the course of conditioning and extinction.^{27,46–50} Human neuroimaging also shows functional specializations for these subfields in memory and affective processes.^{48,51,52} Using subject-specific anatomical segmentations, we probed emotional memory reinstatement along the long axis of the HC in three bilateral subfields: head (anterior HC [aHC]); body; and tail (posterior HC [pHC]). The amygdala was similarly segmented into two bilateral ROIs known to have functional specialization in conditioning and extinction processes: the basolateral amygdala (BLA) and the central nucleus of the amygdala (CeM).⁵³

Hippocampus

No preferential reinstatement was observed for CS+ items from any encoding context in any hippocampal subfield in either healthy adults or individuals with PTSS (all $p_{FDR} \geq 0.45$). However, a linear-mixed effects model revealed a significant three-way interaction: encoding context \times subfield \times group ($\chi^2_{(4)} = 12.8$; $p = 0.012$). The significance of this term suggests subfields of the HC may be sensitive to encoding context in general, but not CS type. As such, we probed reinstatement by encoding context, collapsing across CS+ and CS−. In both groups, the pHC reinstated CS items from the fear conditioning context. In healthy adults, reinstatement of fear memories was stronger than

reinstatement of extinction memories (4.36e−2; [1.40e−2, 7.32e−2]; $p_{FDR} = 0.019$), whereas in adults with PTSS, it was stronger than both extinction memories (4.33e−2; [1.36e−2, 7.29e−2]; $p_{FDR} = 0.019$) and pre-conditioning memories (4.41e−2; [1.45e−2, 7.37e−2]; $p_{FDR} = 0.019$). The body of the HC did not show reinstatement specific to any encoding context (all phase comparisons $p_{FDR} \geq 0.11$). In contrast to the pHC, the aHC preferentially reinstated CS items from extinction more than items from conditioning (0.065; [0.035, 0.094]; $p_{FDR} = 3.36e−4$), although this was only observed in healthy adults. These results suggest a gradient of functional specialization along the long axis of the HC.

We directly tested the dissociation between the aHC and pHC subfields and found a significant double dissociation in healthy adults (significant encoding context \times subfield interaction; $\chi^2_{(1)} = 23.04$; $p = 1.59e−6$). Specifically, the pHC exhibited more fear memory reinstatement than the aHC (0.033; [0.003, 0.063]; $p_{FDR} = 0.038$), and the aHC exhibited more extinction memory reinstatement than the pHC (0.075; [0.046, 0.105]; $p_{FDR} = 2.51e−6$; Figure 3). This double dissociation was not observed in the PTSS group (no significant encoding context \times subfield interaction; $\chi^2_{(1)} = 1.80$; $p = 0.19$). In this group, fear memories were biased toward the pHC (0.034; [0.004, 0.063]; $p_{FDR} = 0.038$), but there was no preference between the aHC and pHC for extinction memories (−0.004; [−0.034, 0.026]; $p_{FDR} = 0.80$). The lack of extinction reinstatement in the aHC further supports the idea that the neural organization of safety memories is dysregulated in PTSS.

As in the mPFC, we directly tested whether the pattern of emotional memory reinstatement observed along the long axis of the HC differed between groups; that is, we compared the reinstatement in aHC versus pHC for each phase between groups. As in the mPFC, the groups did not differ in their patterns of fear memory reinstatement (−5.84e−4; [−0.043, 0.041]; $p_{FDR} = 0.98$); however, there was a significant difference between groups in the reinstatement of extinction memories along the long axis of the HC (0.079; [0.037, 0.121]; $p_{FDR} = 4.37e−4$).

Amygdala

We also probed the subfields of the amygdala for preferential reinstatement of CS+ items. However, none was observed for any encoding context in any subfield, in either group (all $p_{FDR} \geq 0.64$). In addition, we did not observe any significant main effects or interactions in a linear mixed-effects model and thus did not perform other follow-up tests.

MTL activity at retrieval predicts dissociable reinstatement in the mPFC

Univariate activity

Our *a priori* analysis in the mPFC showed that healthy adults exhibited a double dissociation of emotional memory reinstatement. What determines in which area of the mPFC a particular item is reinstated? The HC and amygdala both contain discrete but spatially intermixed populations of neurons that code for fear and extinction.^{10,32,54} Shifts in activity between these populations balance the behavioral expression of emotional memories, in part through their differing long-range connections with the mPFC.^{10,23,27} Regions that exhibit bidirectional control over the expression of emotional memories could be crucial for proper regulation of fear and extinction in humans. Thus, on a trial-by-trial basis, we assessed whether neural activity in the

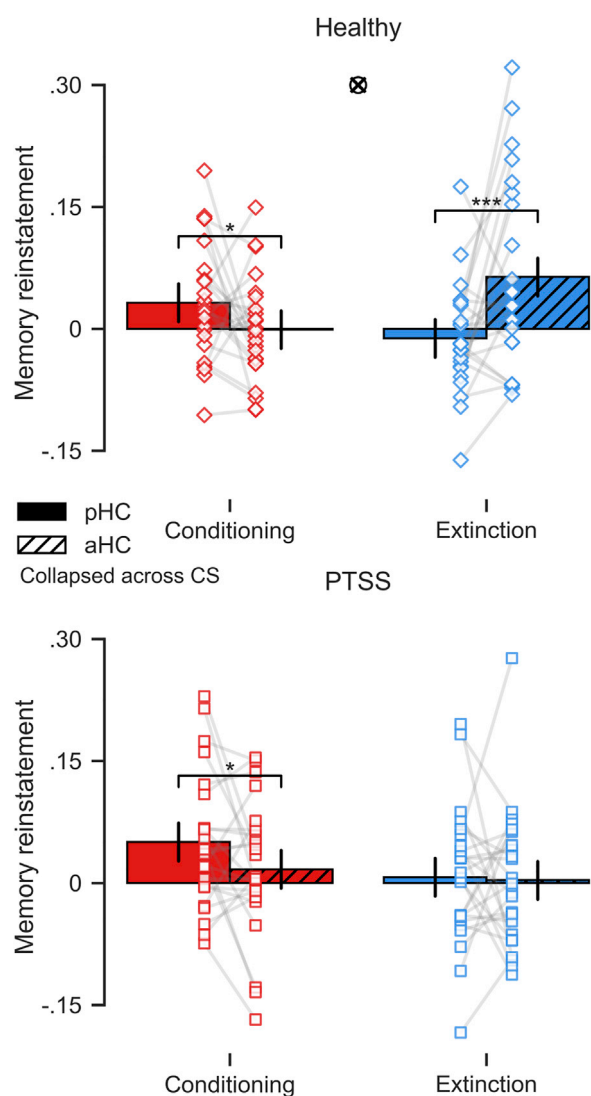


Figure 3. Reinstatement of emotional memories along the long axis of the hippocampus

Reinstatement was collapsed across CS+ and CS- by encoding context in hippocampal subfields. Error bars indicate 95% CI of marginal means. Phase-specific reinstatement was observed in the pHC and aHC, but not the body of the hippocampus (data not shown). ***p < 0.001; *p < 0.05 FDR corrected. Top: healthy adults exhibited a double dissociation of reinstatement. Bottom: in adults with PTSS, the pHC subfield exhibited more conditioning reinstatement than the aHC.

subfields of the HC and amygdala predicted the location of reinstatement between our two mPFC regions (vmPFC and dACC). We restricted our analysis to CS items from conditioning and extinction as our time points of interest.

We found that all subfields were significant predictors of reinstatement location, such that increases in MTL activity at the time of memory retrieval predicted more reinstatement in the dACC (pHC: $X^2_{(1)} = 54.7$, $p = 1.38e-13$, slope = $-1.8e-3$; HC body: $X^2_{(1)} = 68.2$, $p = 1.48e-16$, slope = $-2.49e-3$; aHC: $X^2_{(1)} = 46.8$, $p = 8.00e-12$, slope = $-1.7e-3$; BLA: $X^2_{(1)} = 26.7$, $p = 2.39e-7$, slope = $-1.45e-3$; CeM: $X^2_{(1)} = 19.5$,

$p = 1.01e-5$, slope = $-6.90e-4$). Additionally, we observed several interactions in HC subfields, such that this effect was stronger for all CS+ items in the pHC compared to CS- (pHC \times CS type interaction: $X^2_{(1)} = 11.2$; $p = 8.3e-4$), and was selective for conditioning CS+ items in the body of the hippocampus (significant HC body \times CS type \times encoding context interaction: $X^2_{(1)} = 5.46$; $p = 0.019$).

MTL reinstatement

Having established that overall activity in the MTL predicts more reinstatement in the dACC, we next conducted a similar set of analyses in which trial-by-trial reinstatement was used to predict the mPFC difference in reinstatement. The hypothesis for what MTL reinstatement will predict is not automatically the same as univariate activity, as the information present in a spatial pattern of activity differs from the mean activity across that pattern. Item-specific memory reinstatement in three subfields was predictive of reinstatement in different regions of the mPFC (Figure 4). Greater reinstatement in the pHC ($X^2_{(1)} = 4.64$; $p = 0.031$; slope = -0.060) and CeM ($X^2_{(1)} = 8.49$; $p = 0.004$; slope = -0.065) was associated with a bias toward reinstatement in the dACC. In contrast, greater reinstatement in the aHC ($X^2_{(1)} = 11.1$; $p = 8.51e-4$; slope = 0.091) was associated with a bias toward reinstatement in the vmPFC. There were no significant interactions with encoding context, CS type, or group for any of these subfields. Finally, reinstatement in the body of the hippocampus and the BLA did not predict mPFC reinstatement location.

Separable influence of the aHC

We found that univariate and multivariate signals from the aHC predict opposite biases in mPFC reinstatement during memory retrieval. Greater mean activity in the aHC predicted a bias in reinstatement to the dACC, while greater reinstatement in the same region predicted a bias to the vmPFC. Consistent with the proposition that the aHC exerts bidirectional control over the expression of fear and extinction, we found that both neural signatures were independently predictive of cortical reinstatement when combined into a single model (univariate: $X^2_{(1)} = 42.5$, $p = 7.1e-11$, slope = $-1.65e-3$; reinstatement: $X^2_{(1)} = 5.56$, $p = 0.018$, slope = 0.067), with no significant interactions with either predictor.

DISCUSSION

Extinction learning can build a memory of safety to countervail retrieval and expression of the original fear association. However, an adaptive memory system should preserve the original fear memory, as an experience of safety does not necessarily render a stimulus harmless. These opposing associations should therefore be stored to allow for the appropriate behavior in a given context.⁵⁵ Neurobiological research in rodents is beginning to reveal the structure of this organization within and between discrete brain regions by quantifying overlaps in activity during memory formation and expression.^{6,56,57} Using multivoxel pattern similarity analysis of overlapping encoding-to-retrieval activity in human neuroimaging, we were able to identify a divided organization of fear and extinction memories in the mPFC and hippocampus. Specifically, extinction memories were reinstated in the vmPFC and aHC, while fear memories were reinstated in the dACC and pHC. Individuals with PTSS exhibited a similar pattern of fear memory reinstatement. However,

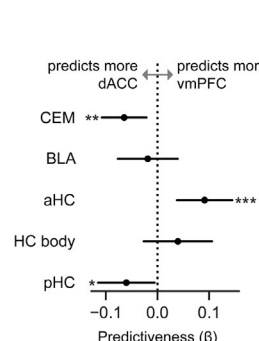
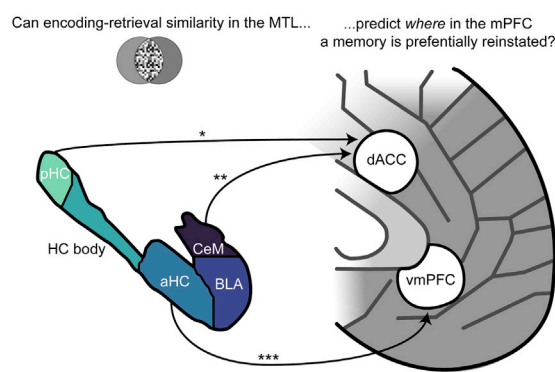


Figure 4. MTL reinstatement predicts mPFC reinstatement location

For hippocampal and amygdalar ROIs, reinstatement was used to predict the vmPFC – dACC difference in reinstatement. Left: stylized representations of the MTL and mPFC are shown, with arrows indicating significant predictions. Right: point estimates and 95% CI of slopes are shown. ***p < 0.001; **p < 0.01; *p < 0.05.

they surprisingly misallocated extinction memories to a region associated with fear memory reinstatement in healthy participants. Across both groups, we observed that various neural signals from the MTL predicted the location of cortical reinstatement of emotional memories in mPFC. These results bridge increasing evidence from rodent neurophysiology for the divided organization of opposing associative memories and provide new insights into how disorganization in these neural representations may contribute to psychiatric disorder.

Previous findings from rodents show the PL is necessary for long-term retrieval and expression of conditioned fear.^{8,58} The PL receives inputs from sensory cortices, thalamus, and other PFC regions, in addition to reciprocal connections with the amygdala and hippocampus.⁵⁹ These connections allow the PL to integrate information from the external environment as well as internal states to flexibly guide behavior in potentially threatening situations. Here, we found that the dACC reinstates activity patterns unique to the formation of associative fear memories, confirming a role for this structure in the organization of long-term fear memories in the human brain. A whole brain searchlight analysis also revealed reinstatement of fear memories in the anterior insula, which together with the dACC are hubs of the salience network.⁶⁰ Collectively, fear memory representations appear distributed across cortical and subcortical networks that may code for unique aspects of the fear experience.^{19,61} Orchestration between these regions likely determines retrieval of fear memory over extinction memory.

The rodent IL is necessary for the long-term extinction memory retention²⁴ and is inhibited by the ventral HC (vHC) during fear renewal.²⁷ Here, we found that the vmPFC reinstates activity patterns unique to the formation of extinction memories in the healthy adult brain. Notably, univariate human neuroimaging evidence for the involvement of the vmPFC in extinction learning and recall has been limited and mixed.³¹ The present findings thus help bridge extensive evidence from rodents to humans on the role of this region in organizing extinction memory to inhibit retrieval and expression of fear. We also found that individuals with PTSS displayed dysregulated organization of fear and extinction reinstatement in the mPFC. Specifically, the dACC exhibited reinstatement of memories formed during extinction, with no such reinstatement in the vmPFC. Critically, behavioral performance of within-session extinction learning was equivalent between groups, and both groups remembered an equivalent number of items from extinction. Thus, differences in neural reinstatement of extinction appears to reflect an

underlying distinction in how these memories are formed and retrieved and do not merely recapitulate an observable behavioral deficit. This suggests that individuals with a history of trauma may utilize a different, and ultimately maladaptive, neural mechanism for fear reduction during within-session extinction learning that bypasses formation of a long-term extinction memory in the vmPFC. Interestingly, evidence from rodent studies shows the IL is not required for within-session extinction, only for successful extinction retrieval.²⁴ However, stimulation of the vmPFC during or after extinction learning improves extinction retention.^{24,62–65} The inability to form an extinction memory in the vmPFC during learning may therefore be a critical factor in extinction retrieval deficits observed in PTSD.^{1,2} Likewise, the misallocation of extinction-specific memories to the dACC, rather than the vmPFC, may bias the retrieval and expression of fear associations following extinction, contributing to fear relapse. These provide potential targets to strengthen extinction memory for clinical purposes.

We also found divided organization of fear and extinction along the long axis of the hippocampus. Neural reinstatement in the hippocampus was sensitive to the temporal context of encoding (fear versus extinction) rather than the valence of the CS (CS+ versus CS-). This contextual specificity aligns with the role of the hippocampus in forming contextual representation in associative learning⁶⁶ and exerting contextual control of extinction retrieval through connections with the mPFC.^{27,67} The hippocampus maintains competing representations of fear and extinction memory in distinct neural populations in the dentate gyrus³² and CA1.⁶⁸ Whether there is a division in dorsal and ventral regions in the representation of fear versus extinction memory is less clear. This organization is likely determined by dissociable connectivity with subregions of the mPFC.^{11,27,46–50,69} Our results suggest that the pHc is involved in the retrieval of fear memories, as both groups displayed selective reinstatement in the pHc for items encoded during fear conditioning. Additionally, neural reinstatement in the pHc, as well as univariate activity, predicted a bias in mPFC reinstatement toward the dACC. The aHC, in contrast, showed selective reinstatement for items encoded in the extinction context. Further analysis showed that the aHC serves a dual role in retrieval of fear and extinction memory. On one hand, neural reinstatement in the aHC predicted reinstatement in the vmPFC, suggesting a network for extinction memory organization. On the other hand, univariate activity in the aHC during memory retrieval predicted reinstatement in the dACC, consistent with a separate network that may facilitate retrieval of associative fear memories. The aHC therefore appears well situated for integrating contextual

information and gating retrieval of the fear or extinction memory through connections with the dACC or vmPFC, respectively.

Given considerable evidence of fear engram reactivation in the rodent BLA,⁵⁷ it is notable that we did not observe reinstatement in the human amygdala. One possibility is that participants were not under threat at retrieval, limiting involvement of the amygdala for behavioral fear expression. However, there was a lack of amygdala involvement at encoding as well, consistent with meta-analyses of fMRI human fear conditioning.^{28,31,70} The limited spatial resolution of fMRI is perhaps to blame for the inability to separate reactivation of sparse neural population coding for both fear and extinction memories,⁷¹ as well as the CS+ and CS-⁷². Although we did not observe preferential CS+ reinstatement in the amygdala, univariate activity in the amygdala, as well as reinstatement in the CeM, predicted reinstatement occurring in the dACC rather than the vmPFC (Figure 4). This is consistent with the idea that reciprocal connections between the amygdala and mPFC organize the storage and retrieval of fear memories.⁶

Much of the recent progress on the neuroscience of fear and extinction has utilized activity-dependent functional labeling to identify the neural organization of opposing memories.^{6,19} Prior human neuroimaging using univariate approaches has broadly confirmed the separation of fear and extinction memories in the mPFC,^{12–15} although recent meta-analyses show the vmPFC is not always strongly activated during extinction learning or retrieval.³¹ Using a multivariate approach to compare encoding-retrieval similarity, we provide evidence for dissociable neural reinstatement of fear and extinction representations in the human brain based on the context in which these memories were formed. These results extend a conceptual framework of engram-like representations and more broadly bolster the use of multivariate pattern analyses to translate cutting-edge advances from the neurobiology of fear and extinction to humans.^{42,73–75} The hybrid episodic and conditioning design afforded us simultaneous access to isolate memories that normally exert reciprocal inhibition during traditional tests of an extinguished memory (e.g. spontaneous recovery). Selective neural reinstatement of competing memories formed under different temporal contexts is predicted by the encoding-specificity principle⁷⁶ and neural reinstatement of episodic memory in human neuroimaging^{34,35} but has not previously been shown for fear and extinction memory in humans. This design may be applied to future work in humans seeking to assess the efficacy of protocols that enhance extinction⁷⁷ or modify the underlying fear memory trace through reconsolidation updating.⁷⁸ A further possibility to extend this work is to target engagement of activity patterns unique to formation of an extinction memory in distributed networks through closed-loop decoded neurofeedback^{79,80} to create an enduring memory of safety. In this way, more precise localization of networks involved in organizing fear and extinction memory could ultimately lead to better treatments of psychiatric disorders like PTSD.

STAR★METHODS

Detailed methods are provided in the online version of this paper and include the following:

• KEY RESOURCES TABLE

• RESOURCE AVAILABILITY

- Lead contact
- Materials availability
- Data and code availability

• EXPERIMENTAL MODEL AND SUBJECT DETAILS

- Participants

• METHOD DETAILS

- Stimuli
- Task
- Functional MRI acquisition
- Image preprocessing
- Region of interest selection
- Multivariate pattern analysis
- Whole-brain searchlight

• QUANTIFICATION AND STATISTICAL ANALYSIS

SUPPLEMENTAL INFORMATION

Supplemental information can be found online at <https://doi.org/10.1016/j.cub.2021.11.004>.

ACKNOWLEDGMENTS

This work was supported by NIH grants F31MH124360 to A.C.H., R01EY028746 to J.A.L.-P., and R01MH122387 and R00MH106719 to J.E.D.

AUTHOR CONTRIBUTIONS

A.C.H., J.E.D., and J.A.L.-P. conceived of and designed the fMRI experiment. A.C.H. and M.M. implemented the fMRI experiment and collected the data. A.C.H. preprocessed and analyzed the data and visualized results. A.C.H., J.E.D., and J.A.L.-P. wrote the original draft of the manuscript. A.C.H., M.R.D., J.E.D., and J.A.L.-P. reviewed and edited the final draft of the manuscript.

DECLARATION OF INTERESTS

The authors declare no competing interests.

Received: June 25, 2021

Revised: September 28, 2021

Accepted: November 2, 2021

Published: November 22, 2021

REFERENCES

1. Lissek, S., and van Meurs, B. (2015). Learning models of PTSD: theoretical accounts and psychobiological evidence. *Int. J. Psychophysiol.* 98, 594–605.
2. Pitman, R.K., Rasmusson, A.M., Koenen, K.C., Shin, L.M., Orr, S.P., Gilbertson, M.W., Milad, M.R., and Liberzon, I. (2012). Biological studies of post-traumatic stress disorder. *Nat. Rev. Neurosci.* 13, 769–787.
3. Johansen, J.P., Cain, C.K., Ostroff, L.E., and LeDoux, J.E. (2011). Molecular mechanisms of fear learning and memory. *Cell* 147, 509–524.
4. Liu, X., Ramirez, S., Pang, P.T., Puryear, C.B., Govindarajan, A., Deisseroth, K., and Tonegawa, S. (2012). Optogenetic stimulation of a hippocampal engram activates fear memory recall. *Nature* 484, 381–385.
5. Rashid, A.J., Yan, C., Mercaldo, V., Hsiang, H.L., Park, S., Cole, C.J., De Cristofaro, A., Yu, J., Ramakrishnan, C., Lee, S.Y., et al. (2016). Competition between engrams influences fear memory formation and recall. *Science* 353, 383–387.
6. Tovote, P., Fadok, J.P., and Lüthi, A. (2015). Neuronal circuits for fear and anxiety. *Nat. Rev. Neurosci.* 16, 317–331.

Current Biology

Article



7. Davis, P., Zaki, Y., Maguire, J., and Reijmers, L.G. (2017). Cellular and oscillatory substrates of fear extinction learning. *Nat. Neurosci.* 20, 1624–1633.
8. Giustino, T.F., and Maren, S. (2015). The role of the medial prefrontal cortex in the conditioning and extinction of fear. *Front. Behav. Neurosci.* 9, 298.
9. Herry, C., Ciochetti, S., Senn, V., Demmou, L., Müller, C., and Lüthi, A. (2008). Switching on and off fear by distinct neuronal circuits. *Nature* 454, 600–606.
10. Senn, V., Wolff, S.B.E., Herry, C., Grenier, F., Ehrlich, I., Gründemann, J., Fadok, J.P., Müller, C., Letzkus, J.J., and Lüthi, A. (2014). Long-range connectivity defines behavioral specificity of amygdala neurons. *Neuron* 81, 428–437.
11. Sierra-Mercado, D., Padilla-Coreano, N., and Quirk, G.J. (2011). Dissociable roles of prelimbic and infralimbic cortices, ventral hippocampus, and basolateral amygdala in the expression and extinction of conditioned fear. *Neuropsychopharmacology* 36, 529–538.
12. Kalisch, R., Korenfeld, E., Stephan, K.E., Weiskopf, N., Seymour, B., and Dolan, R.J. (2006). Context-dependent human extinction memory is mediated by a ventromedial prefrontal and hippocampal network. *J. Neurosci.* 26, 9503–9511.
13. Milad, M.R., Quirk, G.J., Pitman, R.K., Orr, S.P., Fischl, B., and Rauch, S.L. (2007). A role for the human dorsal anterior cingulate cortex in fear expression. *Biol. Psychiatry* 62, 1191–1194.
14. Milad, M.R., Wright, C.I., Orr, S.P., Pitman, R.K., Quirk, G.J., and Rauch, S.L. (2007). Recall of fear extinction in humans activates the ventromedial prefrontal cortex and hippocampus in concert. *Biol. Psychiatry* 62, 446–454.
15. Phelps, E.A., Delgado, M.R., Nearing, K.I., and LeDoux, J.E. (2004). Extinction learning in humans: role of the amygdala and vmPFC. *Neuron* 43, 897–905.
16. Kredlow, M.A., Fenster, R.J., Laurent, E.S., Ressler, K.J., and Phelps, E.A. (2021). Prefrontal cortex, amygdala, and threat processing: implications for PTSD. *Neuropsychopharmacol.* Published online September 20, 2021. <https://doi.org/10.1038/s41386-021-01155-7>.
17. Maren, S., Phan, K.L., and Liberzon, I. (2013). The contextual brain: implications for fear conditioning, extinction and psychopathology. *Nat. Rev. Neurosci.* 14, 417–428.
18. Milad, M.R., and Quirk, G.J. (2012). Fear extinction as a model for translational neuroscience: ten years of progress. *Annu. Rev. Psychol.* 63, 129–151.
19. Frankland, P.W., Josselyn, S.A., and Köhler, S. (2019). The neurobiological foundation of memory retrieval. *Nat. Neurosci.* 22, 1576–1585.
20. Josselyn, S.A., Köhler, S., and Frankland, P.W. (2015). Finding the engram. *Nat. Rev. Neurosci.* 16, 521–534.
21. Burgos-Robles, A., Vidal-Gonzalez, I., and Quirk, G.J. (2009). Sustained conditioned responses in prelimbic prefrontal neurons are correlated with fear expression and extinction failure. *J. Neurosci.* 29, 8474–8482.
22. Burgos-Robles, A., Kimchi, E.Y., Izadmehr, E.M., Porzenheim, M.J., Ramos-Guasp, W.A., Nieh, E.H., Felix-Ortiz, A.C., Namburi, P., Leppa, C.A., Presbrey, K.N., et al. (2017). Amygdala inputs to prefrontal cortex guide behavior amid conflicting cues of reward and punishment. *Nat. Neurosci.* 20, 824–835.
23. Sotres-Bayon, F., Sierra-Mercado, D., Pardilla-Delgado, E., and Quirk, G.J. (2012). Gating of fear in prelimbic cortex by hippocampal and amygdala inputs. *Neuron* 76, 804–812.
24. Do-Monte, F.H., Manzano-Nieves, G., Quiñones-Laracuente, K., Ramos-Medina, L., and Quirk, G.J. (2015). Revisiting the role of infralimbic cortex in fear extinction with optogenetics. *J. Neurosci.* 35, 3607–3615.
25. Klavir, O., Prigge, M., Sarel, A., Paz, R., and Yizhar, O. (2017). Manipulating fear associations via optogenetic modulation of amygdala inputs to prefrontal cortex. *Nat. Neurosci.* 20, 836–844.
26. Milad, M.R., and Quirk, G.J. (2002). Neurons in medial prefrontal cortex signal memory for fear extinction. *Nature* 420, 70–74.
27. Marek, R., Jin, J., Goode, T.D., Giustino, T.F., Wang, Q., Acca, G.M., Holehonnur, R., Ploski, J.E., Fitzgerald, P.J., Lynagh, T., et al. (2018). Hippocampus-driven feed-forward inhibition of the prefrontal cortex mediates relapse of extinguished fear. *Nat. Neurosci.* 21, 384–392.
28. Fullana, M.A., Harrison, B.J., Soriano-Mas, C., Vervliet, B., Cardoner, N., Ávila-Parcet, A., and Radua, J. (2016). Neural signatures of human fear conditioning: an updated and extended meta-analysis of fMRI studies. *Mol. Psychiatry* 21, 500–508.
29. Harrison, B.J., Fullana, M.A., Via, E., Soriano-Mas, C., Vervliet, B., Martínez-Zalacaín, I., Pujol, J., Davey, C.G., Kircher, T., Straube, B., and Cardoner, N. (2017). Human ventromedial prefrontal cortex and the positive affective processing of safety signals. *Neuroimage* 152, 12–18.
30. Milad, M.R., Quinn, B.T., Pitman, R.K., Orr, S.P., Fischl, B., and Rauch, S.L. (2005). Thickness of ventromedial prefrontal cortex in humans is correlated with extinction memory. *Proc. Natl. Acad. Sci. USA* 102, 10706–10711.
31. Fullana, M.A., Albajes-Eizagirre, A., Soriano-Mas, C., Vervliet, B., Cardoner, N., Benet, O., Radua, J., and Harrison, B.J. (2018). Fear extinction in the human brain: a meta-analysis of fMRI studies in healthy participants. *Neurosci. Biobehav. Rev.* 88, 16–25.
32. Lacagnina, A.F., Brockway, E.T., Crovetti, C.R., Shue, F., McCarty, M.J., Sattler, K.P., Lim, S.C., Santos, S.L., Denny, C.A., and Drew, M.R. (2019). Distinct hippocampal engrams control extinction and relapse of fear memory. *Nat. Neurosci.* 22, 753–761.
33. Johnson, J.D., McDuff, S.G.R., Rugg, M.D., and Norman, K.A. (2009). Recollection, familiarity, and cortical reinstatement: a multivoxel pattern analysis. *Neuron* 63, 697–708.
34. Polyn, S.M., Natu, V.S., Cohen, J.D., and Norman, K.A. (2005). Category-specific cortical activity precedes retrieval during memory search. *Science* 310, 1963–1966.
35. Ritchey, M., Wing, E.A., LaBar, K.S., and Cabeza, R. (2013). Neural similarity between encoding and retrieval is related to memory via hippocampal interactions. *Cereb. Cortex* 23, 2818–2828.
36. Staresina, B.P., Henson, R.N.A., Kriegeskorte, N., and Alink, A. (2012). Episodic reinstatement in the medial temporal lobe. *J. Neurosci.* 32, 18150–18156.
37. Staudigl, T., Vollmar, C., Noachtar, S., and Hanslmayr, S. (2015). Temporal-pattern similarity analysis reveals the beneficial and detrimental effects of context reinstatement on human memory. *J. Neurosci.* 35, 5373–5384.
38. Dunsmoor, J.E., and Kroes, M.C.W. (2019). Episodic memory and Pavlovian conditioning: ships passing in the night. *Curr. Opin. Behav. Sci.* 26, 32–39.
39. Garfinkel, S.N., Abelson, J.L., King, A.P., Sripada, R.K., Wang, X., Gaines, L.M., and Liberzon, I. (2014). Impaired contextual modulation of memories in PTSD: an fMRI and psychophysiological study of extinction retention and fear renewal. *J. Neurosci.* 34, 13435–13443.
40. Milad, M.R., Pitman, R.K., Ellis, C.B., Gold, A.L., Shin, L.M., Lasko, N.B., Zeidan, M.A., Handwerger, K., Orr, S.P., and Rauch, S.L. (2009). Neurobiological basis of failure to recall extinction memory in posttraumatic stress disorder. *Biol. Psychiatry* 66, 1075–1082.
41. Rougemont-Bücking, A., Linnman, C., Zeffiro, T.A., Zeidan, M.A., Lebron-Milad, K., Rodriguez-Romaguera, J., Rauch, S.L., Pitman, R.K., and Milad, M.R. (2011). Altered processing of contextual information during fear extinction in PTSD: an fMRI study. *CNS Neurosci. Ther.* 17, 227–236.
42. Hennings, A.C., McClay, M., Lewis-Peacock, J.A., and Dunsmoor, J.E. (2020). Contextual reinstatement promotes extinction generalization in healthy adults but not PTSD. *Neuropsychologia* 147, 107573.
43. Dunsmoor, J.E., Murty, V.P., Davachi, L., and Phelps, E.A. (2015). Emotional learning selectively and retroactively strengthens memories for related events. *Nature* 520, 345–348.

44. Dunsmoor, J.E., Kroes, M.C.W., Moscatelli, C.M., Evans, M.D., Davachi, L., and Phelps, E.A. (2018). Event segmentation protects emotional memories from competing experiences encoded close in time. *Nat. Hum. Behav.* 2, 291–299.

45. Keller, N.E., and Dunsmoor, J.E. (2019). The effects of aversive-to-appetitive counterconditioning on implicit and explicit fear memory. *Learn. Mem.* 27, 12–19.

46. Bast, T., Zhang, W.N., and Feldon, J. (2003). Dorsal hippocampus and classical fear conditioning to tone and context in rats: effects of local NMDA-receptor blockade and stimulation. *Hippocampus* 13, 657–675.

47. Corcoran, K.A., Desmond, T.J., Frey, K.A., and Maren, S. (2005). Hippocampal inactivation disrupts the acquisition and contextual encoding of fear extinction. *J. Neurosci.* 25, 8978–8987.

48. Meyer, H.C., Odriozola, P., Cohodes, E.M., Mandell, J.D., Li, A., Yang, R., Hall, B.S., Haberman, J.T., Zacharek, S.J., Liston, C., et al. (2019). Ventral hippocampus interacts with prelimbic cortex during inhibition of threat response via learned safety in both mice and humans. *Proc. Natl. Acad. Sci. USA* 116, 26970–26979.

49. Qin, C., Bian, X.-L., Wu, H.-Y., Xian, J.-Y., Cai, C.-Y., Lin, Y.-H., Zhou, Y., Kou, X.-L., Chang, L., Luo, C.-X., and Zhu, D.Y. (2021). Dorsal hippocampus to infralimbic cortex circuit is essential for the recall of extinction memory. *Cereb. Cortex* 31, 1707–1718.

50. Ye, X., Kapeller-Libermann, D., Travaglia, A., Inda, M.C., and Alberini, C.M. (2017). Direct dorsal hippocampal-prelimbic cortex connections strengthen fear memories. *Nat. Neurosci.* 20, 52–61.

51. Cooper, R.A., and Ritchey, M. (2019). Cortico-hippocampal network connections support the multidimensional quality of episodic memory. *eLife* 8, e45591.

52. Poppenk, J., Evensmoen, H.R., Moscovitch, M., and Nadel, L. (2013). Long-axis specialization of the human hippocampus. *Trends Cogn. Sci.* 17, 230–240.

53. Pape, H.C., and Pare, D. (2010). Plastic synaptic networks of the amygdala for the acquisition, expression, and extinction of conditioned fear. *Physiol. Rev.* 90, 419–463.

54. Zhang, X., Kim, J., and Tonegawa, S. (2020). Amygdala reward neurons form and store fear extinction memory. *Neuron* 105, 1077–1093.e7.

55. Moorman, D.E., and Aston-Jones, G. (2015). Prefrontal neurons encode context-based response execution and inhibition in reward seeking and extinction. *Proc. Natl. Acad. Sci. USA* 112, 9472–9477.

56. Letzkus, J.J., Wolff, S.B.E., and Lüthi, A. (2015). Disinhibition, a circuit mechanism for associative learning and memory. *Neuron* 88, 264–276.

57. Reijmers, L.G., Perkins, B.L., Matsuo, N., and Mayford, M. (2007). Localization of a stable neural correlate of associative memory. *Science* 317, 1230–1233.

58. Corcoran, K.A., and Quirk, G.J. (2007). Activity in prelimbic cortex is necessary for the expression of learned, but not innate, fears. *J. Neurosci.* 27, 840–844.

59. Hoover, W.B., and Vertes, R.P. (2007). Anatomical analysis of afferent projections to the medial prefrontal cortex in the rat. *Brain Struct. Funct.* 212, 149–179.

60. Seeley, W.W. (2019). The salience network: a neural system for perceiving and responding to homeostatic demands. *J. Neurosci.* 39, 9878–9882.

61. Wheeler, A.L., Teixeira, C.M., Wang, A.H., Xiong, X., Kovacevic, N., Lerch, J.P., McIntosh, A.R., Parkinson, J., and Frankland, P.W. (2013). Identification of a functional connectome for long-term fear memory in mice. *PLoS Comput. Biol.* 9, e1002853.

62. Dunsmoor, J.E., Kroes, M.C.W., Li, J., Daw, N.D., Simpson, H.B., and Phelps, E.A. (2019). Role of human ventromedial prefrontal cortex in learning and recall of enhanced extinction. *J. Neurosci.* 39, 3264–3276.

63. Haaker, J., Gaburro, S., Sah, A., Gartmann, N., Lonsdorf, T.B., Meier, K., Singewald, N., Pape, H.-C., Morellini, F., and Kalisch, R. (2013). Single dose of L-dopa makes extinction memories context-independent and prevents the return of fear. *Proc. Natl. Acad. Sci. USA* 110, E2428–E2436.

64. Milad, M.R., Vidal-Gonzalez, I., and Quirk, G.J. (2004). Electrical stimulation of medial prefrontal cortex reduces conditioned fear in a temporally specific manner. *Behav. Neurosci.* 118, 389–394.

65. Raji, T., Nummenmaa, A., Marin, M.-F., Porter, D., Furtak, S., Setsompop, K., and Milad, M.R. (2018). Prefrontal cortex stimulation enhances fear extinction memory in humans. *Biol. Psychiatry* 84, 129–137.

66. O'Reilly, R.C., and Rudy, J.W. (2001). Conjunctive representations in learning and memory: principles of cortical and hippocampal function. *Psychol. Rev.* 108, 311–345.

67. Bouton, M.E., Maren, S., and McNally, G.P. (2021). Behavioral and neurobiological mechanisms of pavlovian and instrumental extinction learning. *Physiol. Rev.* 101, 611–681.

68. Tronson, N.C., Schrick, C., Guzman, Y.F., Huh, K.H., Srivastava, D.P., Penzes, P., Guedea, A.L., Gao, C., and Radulovic, J. (2009). Segregated populations of hippocampal principal CA1 neurons mediating conditioning and extinction of contextual fear. *J. Neurosci.* 29, 3387–3394.

69. Twining, R.C., Lepak, K., Kirry, A.J., and Gilman, M.R. (2020). Ventral hippocampal input to the prelimbic cortex dissociates the context from the cue association in trace fear memory. *J. Neurosci.* 40, 3217–3230.

70. Fullana, M.A., Albajes-Eizagirre, A., Soriano-Mas, C., Vervliet, B., Cardoner, N., Benet, O., Radua, J., and Harrison, B.J. (2019). Amygdala where art thou? *Neurosci. Biobehav. Rev.* 102, 430–431.

71. Henry, C., Ferraguti, F., Singewald, N., Letzkus, J.J., Ehrlich, I., and Lüthi, A. (2010). Neuronal circuits of fear extinction. *Eur. J. Neurosci.* 31, 599–612.

72. Ghosh, S., and Chattarji, S. (2015). Neuronal encoding of the switch from specific to generalized fear. *Nat. Neurosci.* 18, 112–120.

73. Bach, D.R., Weiskopf, N., and Dolan, R.J. (2011). A stable sparse fear memory trace in human amygdala. *J. Neurosci.* 31, 9383–9389.

74. Graner, J.L., Stjepanović, D., and LaBar, K.S. (2020). Extinction learning alters the neural representation of conditioned fear. *Cogn. Affect. Behav. Neurosci.* 20, 983–997.

75. Visser, R.M., Scholte, H.S., Beemsterboer, T., and Kindt, M. (2013). Neural pattern similarity predicts long-term fear memory. *Nat. Neurosci.* 16, 388–390.

76. Tulving, E., and Thomson, D.M. (1973). Encoding specificity and retrieval processes in episodic memory. *Psychol. Rev.* 80, 352–373.

77. Dunsmoor, J.E., Niv, Y., Daw, N., and Phelps, E.A. (2015). Rethinking extinction. *Neuron* 88, 47–63.

78. Ressler, R.L., Goode, T.D., Kim, S., Ramanathan, K.R., and Maren, S. (2021). Covert capture and attenuation of a hippocampus-dependent fear memory. *Nat. Neurosci.* 24, 677–684.

79. Taschereau-Dumouchel, V., Cortese, A., Chiba, T., Knotts, J.D., Kawato, M., and Lau, H. (2018). Towards an unconscious neural reinforcement intervention for common fears. *Proc. Natl. Acad. Sci. USA* 115, 3470–3475.

80. Taschereau-Dumouchel, V., Cortese, A., Lau, H., and Kawato, M. (2021). Conducting decoded neurofeedback studies. *Soc. Cogn. Affect. Neurosci.* 16, 838–848.

81. Blevins, C.A., Weathers, F.W., Davis, M.T., Witte, T.K., and Domino, J.L. (2015). The posttraumatic stress disorder checklist for DSM-5 (PCL-5): development and initial psychometric evaluation. *J. Trauma. Stress* 28, 489–498.

82. LeDoux, J.E., and Pine, D.S. (2016). Using neuroscience to help understand fear and anxiety: a two-system framework. *Am. J. Psychiatry* 173, 1083–1093.

83. Tustison, N.J., Avants, B.B., Cook, P.A., Zheng, Y., Egan, A., Yushkevich, P.A., and Gee, J.C. (2010). N4ITK: improved N3 bias correction. *IEEE Trans. Med. Imaging* 29, 1310–1320.

84. Avants, B.B., Epstein, C.L., Grossman, M., and Gee, J.C. (2008). Symmetric diffeomorphic image registration with cross-correlation: evaluating automated labeling of elderly and neurodegenerative brain. *Med. Image Anal.* 12, 26–41.

85. Zhang, Y., Brady, M., and Smith, S. (2001). Segmentation of brain MR images through a hidden Markov random field model and the expectation–maximization algorithm. *IEEE Trans. Med. Imaging* **20**, 45–57.
86. Dale, A.M., Fischl, B., and Sereno, M.I. (1999). Cortical surface-based analysis. I. Segmentation and surface reconstruction. *Neuroimage* **9**, 179–194.
87. Klein, A., Ghosh, S.S., Bao, F.S., Giard, J., Häme, Y., Stavsky, E., Lee, N., Rossa, B., Reuter, M., Chaibub Neto, E., and Keshavan, A. (2017). Mindboggling morphometry of human brains. *PLoS Comput. Biol.* **13**, e1005350.
88. Fonov, V.S., Evans, A.C., McKinstry, R.C., Almlí, C.R., and Collins, D.L. (2009). Unbiased nonlinear average age-appropriate brain templates from birth to adulthood. *Neuroimage* **47**, S102.
89. Greve, D.N., and Fischl, B. (2009). Accurate and robust brain image alignment using boundary-based registration. *Neuroimage* **48**, 63–72.
90. Jenkinson, M., Bannister, P., Brady, M., and Smith, S. (2002). Improved optimization for the robust and accurate linear registration and motion correction of brain images. *Neuroimage* **17**, 825–841.
91. Cox, R.W., and Hyde, J.S. (1997). Software tools for analysis and visualization of fMRI data. *NMR Biomed.* **10**, 171–178.
92. Power, J.D., Mitra, A., Laumann, T.O., Snyder, A.Z., Schlaggar, B.L., and Petersen, S.E. (2014). Methods to detect, characterize, and remove motion artifact in resting state fMRI. *Neuroimage* **84**, 320–341.
93. Behzadi, Y., Restom, K., Liau, J., and Liu, T.T. (2007). A component based noise correction method (CompCor) for BOLD and perfusion based fMRI. *Neuroimage* **37**, 90–101.
94. Satterthwaite, T.D., Elliott, M.A., Gerraty, R.T., Ruparel, K., Loughead, J., Calkins, M.E., Eickhoff, S.B., Hakonarson, H., Gur, R.C., Gur, R.E., and Wolf, D.H. (2013). An improved framework for confound regression and filtering for control of motion artifact in the preprocessing of resting-state functional connectivity data. *Neuroimage* **64**, 240–256.
95. Lanczos, C. (1964). Evaluation of noisy data. *J. SIAM Numer. Anal. Ser. B* **1**, 76–85.
96. Jenkinson, M., Beckmann, C.F., Behrens, T.E., Woolrich, M.W., and Smith, S.M. (2012). FSL. *Neuroimage* **62**, 782–790.
97. Fischl, B. (2012). FreeSurfer. *Neuroimage* **62**, 774–781.
98. Iglesias, J.E., Augustinack, J.C., Nguyen, K., Player, C.M., Player, A., Wright, M., Roy, N., Frosch, M.P., McKee, A.C., Wald, L.L., et al.; Alzheimer's Disease Neuroimaging Initiative (2015). A computational atlas of the hippocampal formation using ex vivo, ultra-high resolution MRI: Application to adaptive segmentation of in vivo MRI. *Neuroimage* **115**, 117–137.
99. Saygin, Z.M., Kliemann, D., Iglesias, J.E., van der Kouwe, A.J.W., Boyd, E., Reuter, M., Stevens, A., Van Leemput, K., McKee, A., Frosch, M.P., et al.; Alzheimer's Disease Neuroimaging Initiative (2017). High-resolution magnetic resonance imaging reveals nuclei of the human amygdala: manual segmentation to automatic atlas. *Neuroimage* **155**, 370–382.
100. Kim, H. (2019). Neural correlates of explicit and implicit memory at encoding and retrieval: A unified framework and meta-analysis of functional neuroimaging studies. *Biol. Psychol.* **145**, 96–111.
101. Mumford, J.A., Turner, B.O., Ashby, F.G., and Poldrack, R.A. (2012). Deconvolving BOLD activation in event-related designs for multivoxel pattern classification analyses. *Neuroimage* **59**, 2636–2643.
102. Mumford, J.A., Davis, T., and Poldrack, R.A. (2014). The impact of study design on pattern estimation for single-trial multivariate pattern analysis. *Neuroimage* **103**, 130–138.
103. Kim, H., Smolker, H.R., Smith, L.L., Banich, M.T., and Lewis-Peacock, J.A. (2020). Changes to information in working memory depend on distinct removal operations. *Nat. Commun.* **11**, 6239.
104. Etzel, J.A., Zacks, J.M., and Braver, T.S. (2013). Searchlight analysis: promise, pitfalls, and potential. *Neuroimage* **78**, 261–269.
105. Kriegeskorte, N., Goebel, R., and Bandettini, P. (2006). Information-based functional brain mapping. *Proc. Natl. Acad. Sci. USA* **103**, 3863–3868.
106. Cox, R.W. (1996). AFNI: software for analysis and visualization of functional magnetic resonance neuroimages. *Comput. Biomed. Res.* **29**, 162–173.
107. Gold, S., Christian, B., Arndt, S., Zeien, G., Cizadlo, T., Johnson, D.L., Flaum, M., and Andreasen, N.C. (1998). Functional MRI statistical software packages: a comparative analysis. *Hum. Brain Mapp.* **6**, 73–84.
108. Talairach, J. (1988). Co-Planar Stereotaxic Atlas of the Human Brain: 3-D Proportional System: An Approach to Cerebral Imaging, First Edition (Thieme).
109. Vallat, R. (2018). Pingouin: statistics in Python. *J. Open Source Softw.* **3**, 1026.
110. Lawrence, M.A. (2016). ez: easy analysis and visualization of factorial experiments. <https://cran.r-project.org/web/packages/ez/index.html>.
111. Singmann, H., Bolker, B., and Westfall, J. (2015). Afex: analysis of factorial experiments. R Package Version 0.15-2. <http://CRAN.R-project.org/package=afex>.
112. Luke, S.G. (2017). Evaluating significance in linear mixed-effects models in R. *Behav. Res. Methods* **49**, 1494–1502.
113. Lenth, R. (2019). Emmeans: estimated marginal means aka least-squares means. <https://cran.r-project.org/web/packages/emmeans/index.html>.

STAR★METHODS

KEY RESOURCES TABLE

REAGENT or RESOURCE	SOURCE	IDENTIFIER
Deposited data		
Deidentified neuroimaging and behavioral data	From PI Joseph E. Dunsmoor ⁴²	OSF: https://doi.org/10.17605/OSF.IO/QEG83
Software and algorithms		
Custom python and R analysis code	This paper	OSF: https://doi.org/10.17605/OSF.IO/QEG83

RESOURCE AVAILABILITY

Lead contact

Further information and requests for resources should be directed to and will be fulfilled by the lead contact Joseph E. Dunsmoor (joseph.dunsmoor@austin.utexas.edu).

Materials availability

This study did not generate any unique reagents.

Data and code availability

- All deidentified neuroimaging and behavioral data have been deposited at OSF and are publicly available as of the date of the publication. The DOI is listed in the [Key resources table](#).
- All custom python and R code used for analysis has been deposited at OSF and is publicly available as of the date of publication. The DOI is listed in the [Key resources table](#).
- Any additional information required to reanalyze the data reported in this paper is available from the lead contact upon request.

EXPERIMENTAL MODEL AND SUBJECT DETAILS

Participants

A total of 48 participants from the community volunteered to complete the two-day functional MRI study. Three additional participants were recruited but did not complete the experiment. Half of the participants (N = 24; 15 female; Mean age = 21) were recruited with the criteria that they have no current or past psychiatric or neurological disorders. The remaining participants (N = 24; 17 female; Mean age = 26) were recruited after responding to flyers seeking volunteers with PTSD. These participants underwent phone screening and completed additional in-person questionnaires to confirm Criterion A trauma exposure on the PTSD checklist for DSM-5 (PCL),⁸¹ as well as the absence of other neurological disorders. All PTSD responding participants reported significant post-trauma symptoms related to a Criterion A trauma, however we refer to this cohort as having post-traumatic stress symptoms (PTSS) as we did not implement a structured diagnostic interview. Given high rates of co-morbid substance use disorder, all PTSS participants were given a urine toxicology screening, and no participants tested positive for illicit drugs or benzodiazepines. Written informed consent was obtained for all participants, and all experimental procedures were approved by the University of Texas at Austin IRB (#2017-02-0094). PCL scores, as well as surveys of anxiety and depression are reported in Hennings et al.⁴²

METHOD DETAILS

Stimuli

Conditioned stimuli were images of animals and tools collected from lifeonwhite.com or other publicly available resources on the internet. Critical to the design of the task, each stimulus was a unique exemplar from its category. For example, there were not two different kinds of “dog” used. Typically phobic animals or threatening tools were excluded (e.g., spiders, snakes, knives). The unconditioned stimulus (US) was a brief (50ms) electric shock delivered to fingers of the left hand. Prior to entering the scanner, the US was calibrated for each participant to a level described as “highly annoying and unpleasant, but not painful.” A BIOPAC STMEPM-MRI module was used to deliver the US (Goleta, CA). During the recognition memory test, all 144 “old” stimuli were shown, in addition to 48 novel lures per category. CSs were presented for 3 s followed by a 4 or 5 s ITI (jittered). Trial order was again pseudorandomized to ensure a balance of CSs from each encoding phase as well as old and new items. Stimulus presentation was controlled using E-Prime 3.0.

Task

Associative learning task

Participants completed an associative learning task in two sessions of about an hour each, roughly 24 hours apart. We note that “fear” can be a misnomer of the emotional construct being studied in research involving human participants.⁸² A better term may be “threat conditioning,” as it better captures both the actual emotional experience of participants and the acquisition of conditioned responses. Nevertheless, we retain the term “fear” to connect the results to the broader field of Pavlovian conditioning across model organisms. For all phases of the associative learning task, images were displayed for 4.5 ± 0.5 s (jittered), and the ITI between trials lasted 6 ± 0.5 s (jittered). The trial order of the CSs was pseudorandomized to ensure no more than 3 CS type were presented in a row. The same pseudorandomized order was used for all subjects, however which phase of the experiment each stimulus was displayed was randomized across participants. Day 1 consisted of pre-conditioning, fear conditioning, and extinction. On Day 1, each phase consisted of 48 trials, 24 animals and 24 tools, for a total of 144 items. During pre-conditioning, participants identified which category each image belonged to (2-alternative forced choice, 2-AFC; animal or tool). During fear conditioning, 50% of the trials from one category (CS+) co-terminated with the US, for a total of 12 CS+US pairings. Images from the other category were never paired with shock (CS-), and the category of the CS+ was counterbalanced across participants. Extinction learning followed fear conditioning, during which no shocks were delivered. Relevant to hypotheses explained in Hennings et al.,⁴² during extinction learning the normal fixation cross displayed during the ITI was replaced with a stream of natural scene images displayed for 1 s each (5, 6, or 7 scenes per ITI). During fear conditioning and extinction on Day 1, participants responded whether or not they expected a shock on each trial (2-AFC; yes or no). Skin-conductance responses were collected during pre-conditioning, fear condition, and extinction. The following day, participants had the electrodes reattached prior to entering the scanner for the fear renewal test (reported in Hennings et al.⁴²).

Recognition memory test

After completing the fear renewal test on Day 2, participants completed a surprise recognition memory test for the items they had seen the previous day. Participants were informed that no shocks would be delivered during the memory test. All 144 old images were included as well as 96 novel foils. The stimuli seen during the fear renewal test were not shown during the recognition memory test. Each image was displayed for 3 s with a 4 or 5 s ITI, and participants indicated whether each image was old (they had seen it the previous day), or new (never seen before). Participants indicated the confidence of their choice by responding the image was definitely old, maybe old, maybe new, or definitely new. The memory test was split into three fMRI runs of equal length, and trial order was again pseudorandomized to ensure a balance of lures and foils of both CS types and encoding phases across the memory runs. Trials during the recognition memory test were removed from analysis if participants failed to make a response within the 3 s window (Mean = 2.5 dropped “old” trials per participant). A perceptual localizer followed the recognition memory test to facilitate MVPA decoding, however this data was not used in the present analyses.

Functional MRI acquisition

Neuroimaging was accomplished using the Siemens Skyra 3T Human MRI scanner located at the Biomedical Imaging Center at the University of Texas at Austin. Functional data were acquired with a 32-channel head-coil, with 3mm isotropic resolution (TR = 2000ms; TE = 29ms; FoV = 228; 48 slices). A multi-band factor of 2 was used with automatic AC/PC alignment. As discussed in Hennings et al.,⁴² due to a computer malfunction, 2 subjects had slightly different acquisition parameters on Day 1 (TR = 2230ms; 66 slices), which were accounted for during preprocessing and analysis. An T1-weighted 3d MPRAGE scan (TR = 1900ms; 1mm isotropic resolution) was collected on Day 1 to aid in functional image registration and region of interest definition.

Image preprocessing

Functional MRI data were processed using *fMRIprep* (v1.5.4), an open source software suite designed to increase reproducibility and develop common best practices for image processing. The following boilerplate has been included unchanged, as recommended by the package maintainers.

Anatomical data preprocessing

The T1-weighted (T1w) image was corrected for intensity non-uniformity (INU) with N4BiasFieldCorrection,⁸³ distributed with ANTs 2.2.0,⁸⁴ and used as T1w-reference throughout the workflow. The T1w-reference was then skull-stripped with a *Nipype* implementation of the *antsBrainExtraction.sh* workflow (from ANTs), using OASIS30ANTS as target template. Brain tissue segmentation of cerebrospinal fluid (CSF), white-matter (WM) and gray-matter (GM) was performed on the brain-extracted T1w using fast (FSL 5.0.9⁸⁵). Brain surfaces were reconstructed using recon-all (FreeSurfer 6.0.1⁸⁶), and the brain mask estimated previously was refined with a custom variation of the method to reconcile ANTs-derived and FreeSurfer-derived segmentations of the cortical gray-matter of Mindboggle.⁸⁷ Volume-based spatial normalization to one standard space (MNI152NLin2009cAsym) was performed through nonlinear registration with *antsRegistration* (ANTs 2.2.0), using brain-extracted versions of both T1w reference and the T1w template. The following template was selected for spatial normalization: *ICBM 152 Nonlinear Asymmetrical template version 2009c*.⁸⁸

Functional data preprocessing

For each of the 9 BOLD runs found per subject (across all tasks and sessions), the following preprocessing was performed. First, a reference volume and its skull-stripped version were generated using a custom methodology of *fMRIprep*. Susceptibility

distortion correction (SDC) was omitted as no field maps were collected. The BOLD reference was then co-registered to the T1w reference using bbregister (FreeSurfer) which implements boundary-based registration.⁸⁹ Co-registration was configured with six degrees of freedom. Head-motion parameters with respect to the BOLD reference (transformation matrices, and six corresponding rotation and translation parameters) are estimated before any spatiotemporal filtering using mcflirt (FSL 5.0.9⁹⁰). BOLD runs were slice-time corrected using 3dTshift from AFNI 20160207.⁹¹ The BOLD time-series (including slice-timing correction when applied) were resampled onto their original, native space by applying the transforms to correct for head-motion. These resampled BOLD time-series will be referred to as *preprocessed BOLD in original space*, or just *preprocessed BOLD*. The BOLD time-series were resampled into standard space, generating a *preprocessed BOLD run in MNI152NLin2009cAsym space*. First, a reference volume and its skull-stripped version were generated using a custom methodology of fMRIprep. Several confounding time-series were calculated based on the *preprocessed BOLD*: framewise displacement (FD), DVARS and three region-wise global signals. FD and DVARS are calculated for each functional run, both using their implementations in Nipype (following the definitions by Power et al.⁹²). The three global signals are extracted within the CSF, the WM, and the whole-brain masks. Additionally, a set of physiological regressors were extracted to allow for component-based noise correction (*CompCor*⁹³). Principal components are estimated after high-pass filtering the *preprocessed BOLD* time-series (using a discrete cosine filter with 128 s cut-off) for the two *CompCor* variants: temporal (tCompCor) and anatomical (aCompCor). tCompCor components are then calculated from the top 5% variable voxels within a mask covering the subcortical regions. This subcortical mask is obtained by heavily eroding the brain mask, which ensures it does not include cortical GM regions. For aCompCor, components are calculated within the intersection of the aforementioned mask and the union of CSF and WM masks calculated in T1w space, after their projection to the native space of each functional run (using the inverse BOLD-to-T1w transformation). Components are also calculated separately within the WM and CSF masks. For each CompCor decomposition, the k components with the largest singular values are retained, such that the retained components' time series are sufficient to explain 50 percent of variance across the nuisance mask (CSF, WM, combined, or temporal). The remaining components are dropped from consideration. The head-motion estimates calculated in the correction step were also placed within the corresponding confounds file. The confound time series derived from head motion estimates and global signals were expanded with the inclusion of temporal derivatives and quadratic terms for each.⁹⁴ Frames that exceeded a threshold of 0.5 mm FD or 1.5 standardized DVARS were annotated as motion outliers. All resamplings can be performed with a *single interpolation step* by composing all the pertinent transformations (i.e., head-motion transform matrices, susceptibility distortion correction when available, and co-registrations to anatomical and output spaces). Gridded (volumetric) resamplings were performed using antsApplyTransforms (ANTS), configured with Lanczos interpolation to minimize the smoothing effects of other kernels.⁹⁵ Non-gridded (surface) resamplings were performed using mri_vol2surf (FreeSurfer).

Region of interest selection

The dACC, vmPFC, hippocampus, and amygdala were selected *a priori* to test for the presence of encoding specificity of fear and extinction memories. Prefrontal ROIs were based on peak coordinates previously reported in literature. Specifically, dACC coordinates (MNI 1, 21, 27) were taken from Milad et al.¹³ in which a univariate contrast of CS+ > CS- during fear conditioning was used. vmPFC coordinates (MNI -4, 34, -6) were taken from an fMRI meta-analysis of extinction recall,³¹ using a univariate contrast of CS+ extinguished > CS+ unextinguished. For each ROI, a sphere was drawn around the coordinates with a radius of 10mm, and was then restricted to gray matter using a gray matter probability mask with a threshold of 50%. The masks were then warped to subject space to achieve native functional resolution (3mm³) for multivariate analyses. Registration was accomplished using flirt using 12 degrees of freedom and nearest neighbor interpolation for each binary mask (FSL 5.0.9⁹⁶).

The hippocampus and amygdala were masked and segmented into subfields using Freesurfer's segmentHA_T1 on the preprocessed T1w anatomical images from recon-all (Freesurfer 7.0⁹⁷⁻⁹⁹). The hippocampus was segmented into head (anterior), body, and tail (posterior) subfields along the long axis. The amygdala was segmented into the basolateral (BLA), and central nucleus (CeM) subfields. The segmentations were first warped from Freesurfer native space to T1w space, and then from T1w space to standard space using antsApplyTransforms and the transforms calculated by fMRIprep for each subject. Multilabel interpolation was used to ensure that the segmentations did not overlap, and were then resampled into 3mm³ resolution using ResampleImage from ANTs. Binary masks were then created for each segmentation using fslmaths.

In addition to these *a priori* ROIs, we also probed emotional reinstatement in the anterior insula and the precuneus based on the results from our whole-brain searchlight. The anterior insula was defined bilaterally using coordinates from a meta-analysis of fear conditioning using a CS+ > CS- univariate contrast (MNI lh: -40, 18, -2; rh: 40, 16, 2).²⁸ The radius for each sphere was set to 8mm to better match the number of voxels selected in our midline ROIs. The precuneus was defined from a recent fMRI meta-analysis of episodic memory studies using a contrast for retrieval success (i.e., hits > correct rejection) with a radius of 10mm (MNI -9, -71, 27).¹⁰⁰ The anterior insula and precuneus ROIs were then restricted to gray matter voxels and registered to each subject as above with our mPFC ROIs.

Multivariate pattern analysis

After preprocessing with fMRIprep, we computed a LS-S style betaseries to facilitate the encoding-retrieval similarity analysis.^{101,102} For each scanner run, trial-specific beta images are computed iteratively using a general linear model (GLM) which models a single trial of interest and all other trials as regressors of no interest based on trial type (separate CS+/- no interest regressors). In addition to

the betaseries images, we also generated conventional average activity estimates for CS+ and CS- separately from each phase of learning on Day 1, (i.e., all CS+ in one regressor of interest). For GLMs of fear conditioning, the US was modeled as a 0 duration event and treated as a regressor of no interest. All GLM estimation was accomplished using FSL FEAT, prewhitening was used, and spatial smoothing was not applied in order to respect the boundaries of our *a priori* ROIs. In addition to the preprocessing applied by fMRIprep, several signals were included as confounds to be removed during GLM estimation, including the first principle component of the estimated physiological noise (aCompCor), framewise displacement, 6 standard motion parameters, and the discrete cosine-basis regressors calculated by fMRIprep for high-pass filtering.

The encoding-retrieval similarity analysis was implemented in custom Python code. The goal of this analysis was to directly compare multi-voxel patterns observed during encoding and retrieval of a specific stimulus in each ROI on a per-participant basis. In order to reduce noise prior to estimating pattern similarity, the LS-S beta images were weighted (multiplied) by the overall univariate estimate of the corresponding CS type from encoding^{42,103} (e.g., all images of extinction CS+s from encoding and retrieval were weighted by the univariate estimate of extinction CS+ activity during encoding). For each ROI, encoding-retrieval similarity was then taken as the Pearson's correlation between the two beta images for a given stimulus, one from encoding and one from retrieval. Pearson's r values were Fisher-z transformed and submitted to statistical analysis.

Whole-brain searchlight

The searchlight analysis^{104,105} was accomplished using the *nilearn* package in Python using the functional resolution images (3mm³) registered to MNI space. Images were prepared as described above, and then each pair of beta images from encoding and retrieval was submitted to a whole-brain searchlight analysis in which a Pearson's correlation was iteratively computed in every sphere (radius = 6mm) in the brain. The resulting maps were Fisher-z transformed, and averaged by CS type and encoding context for each subject. For each encoding context, the difference between the average CS+ – CS- maps was taken and analyzed using AFNI (v20.2.18).^{91,106,107} Specifically, 3dttest++ was used to test the CS+ – CS- difference against 0 for each encoding context and for each group. The analysis was restricted to voxels that had $\geq 50\%$ gray matter probability. Family-wise error correction was achieved using the -Clustsim option, which uses permutation testing to simulate the null distribution of the data in order to determine the threshold necessary to observe significant clusters. Clusters were extracted using 3dClusterize using a peak threshold of $p < 0.001$ (one-tailed CS+ – CS-), and a cluster threshold corresponding to $p < 0.05$ using full voxel connectivity. The size of the cluster necessary to reach this threshold ranged from 16–21 across the 4 maps. The coordinates of the peak voxel in each cluster were submitted to the AFNI function whereami to obtain anatomical labels based on the Talairach-Tournoux Atlas.¹⁰⁸ The *pysurfer* package in Python was used to resample and slightly smooth (FWHM = 1mm) the cluster maps onto the cortical surface for display purposes.

QUANTIFICATION AND STATISTICAL ANALYSIS

With the exception of the whole-brain searchlight analysis (see above), all statistical tests are reported as two-tailed, and all estimates of error are given as parametric 95% confidence intervals (i.e., $1.96 \times$ standard error of the mean). Behavioral data was analyzed using the *pingouin*¹⁰⁹ package in Python and the *ez*¹¹⁰ package in R. As discussed in Hennings et al.⁴² due to technical errors four participants (two in each group) are missing SCR data from extinction. SCR was square-root transformed prior to analysis and analyzed using paired and independent samples t tests (see Hennings et al.⁴² for description of SCR scoring method). 2-AFC shock expectancy from conditioning and extinction was coded as 1 = expect, and 0 = do not expect, and analyzed using paired and independent samples t tests. As our neural analysis focused on the reinstatement of previously encoded items, the analysis of recognition memory focused on high-confidence hits (i.e., definitely old responses). Hit rates were submitted to a mixed ANOVA with within subject factors of *encoding context* and *CS type*, and a between-subjects factor of *group*.

All other statistical analyses were accomplished with linear mixed effects models using the *afex*¹¹¹ package in R with maximum likelihood estimation. Encoding-retrieval similarity was analyzed on a trial wise basis, and the model included fixed effects of CS type, encoding context, subfield, and group, as well as a random intercept of subject (*reinstatement ~CS type * encoding context * subfield * group + (1|subject)*). The subfield term here represents the vmPFC/dACC when modeling reinstatement in the mPFC, and the subdivisions of the hippocampus and amygdala for reinstatement in those structures. Significance of the main effects and interactions of the fixed effects was evaluated using Chi-square tests, comparing the log-likelihoods of a model with and without the term of interest.¹¹² All possible interactions were modeled, and the highest order interaction is reported for a given effect when relevant. When testing the double dissociations of reinstatement in the mPFC and hippocampus, data was restricted to CS items from conditioning and extinction, and a separate model was fit for each group (without the *group* term). All planned and post hoc contrasts were accomplished using the *emmeans*¹¹³ package in R. Asymptotic degrees of freedom were used, as in general the number of observations in each model was quite large (between $\sim 4,000$ up to $\sim 20,000$). Parametric 95% confidence intervals of the differences are reported along with FDR corrected P values using the *p.adjust* function in R. FDR correction was applied to each family of tests in each group of ROIs; for example, FDR correction was applied to the 12 tests of CS+ – CS- reinstatement in the mPFC (2 ROIs, 3 contexts, 2 groups). FDR correction was also applied at the next level of analysis; for example, the 4 cross-ROI comparisons of CS+ – CS- reinstatement in the mPFC (2 ROIs, 2 groups).

Linear mixed-effects models were also used to evaluate whether MTL activity predicted the difference in mPFC reinstatement ($\text{vmPFC} - \text{dACC reinstatement} \sim \text{predictor} * \text{CS type} * \text{encoding context} * \text{group} + (1|\text{subject})$). In all cases our analysis focused only on the main effect and interactions of *predictor*, which was iteratively univariate activity or local reinstatement from all MTL ROIs. The same procedure was used to evaluate the separable contributions of univariate activity and reinstatement in the aHC; both neural signals were entered as predictors in a single model. Significance of main effects and interactions was again determined using log-likelihood ratio tests and point estimates and parametric 95% confidence intervals of the slopes were obtained using the *emtrends* function from *emmeans*.